High Resolution Electronic Spectroscopy of Vibrationally Hot Bands of Benzimidazole

ARTICLE *in* THE JOURNAL OF PHYSICAL CHEMISTRY A · NOVEMBER 2013

Impact Factor: 2.69 · DOI: 10.1021/jp408755q · Source: PubMed

THE JOURNAL OF PHYSICAL CHEMISTRY A

Article

pubs.acs.org/JPCA

High Resolution Electronic Spectroscopy of Vibrationally Hot Bands of Benzimidazole

Christian Brand,† Josefin Rolf, Martin Wilke, and Michael Schmitt*

Institut für Physikalische Chemie I, Heinrich-Heine-Universität, D-40225 Düsseldorf, Germany

Supporting Information

ABSTRACT: Rotationally resolved electronic spectra of seven vibrationally excited bands in the electronic spectrum of benzimidazole have been measured and analyzed. From the vibrational contributions to the rotational constants, an assignment of the hot bands could be made on the basis of anharmonic corrections to the harmonic normal modes and by using the information contained in the Duschinsky matrix calculated by second order coupled cluster (CC2) theory. Fluorescence emission and (hot) absorption spectra of benzimidazole from Jalviste and Treshchalov [*Chem. Phys.* **1993**, *172*, 325] have been simulated using Franck−Condon integrals obtained from CC2 optimized geometries and Hessians.

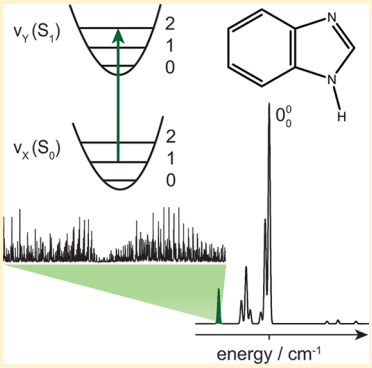

1. INTRODUCTION

Hot bands appearing in vibrationally resolved electronic spectra are frequently regarded as a nuisance. They complicate the assignment of the observed features to the normal modes and their combinations/overtones. However, they contain valuable information on the changes of the potential energy surface upon electronic excitation. Rotationally resolved electronic spectroscopy of hot bands in combination with anharmonic calculations has some appealing features: it allows investigation of spectroscopic features, which are not observable otherwise. Thermally populated out of plane vibrations (symmetry a'') of planar C_s-symmetric molecules like benzimidazole (cf. Figure 1) can be studied since the transition dipole moment lies in the aromatic plane. Furthermore, diagonal transitions (Q_1^1) are often very intense and can be analyzed with a good signal-to-noise ratio.

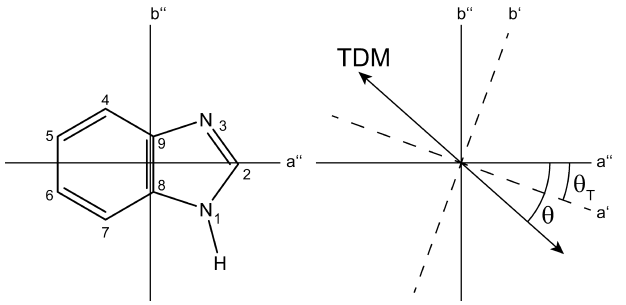

Figure 1. Atomic numbering of 1*H*2*H*-benzimidazole in its principle axis frame. The definition of the negative angle of the TDM angle θ and the axis reorientation angle θ_T are shown on the right.

In the present article, we study thermally populated vibrational hot bands of benzimidazole using rotationally resolved electronic spectroscopy. Fluorescence emission spectra of benzimidazole via excitation of various vibronic bands and a fluorescence excitation spectrum have been presented by Jalviste and Treshchalov.[1] Their fluorescence excitation spectrum shows a wealth of vibrational hot bands, which can also be found in the resonance enhanced multiphoton spectra of Jacoby et al.[2] Velino et al.[3] measured the microwave spectrum of benzimidazole and reported vibrationally averaged rotational constants of two vibrationally excited states at 180 and 210 cm^{-1}. A band contour analysis of benzimidazole in the vapor phase was conducted by Cané et al.[4] Later, Berden et al.[5] presented the rotationally resolved spectrum of the origin of benzimidazole in a cold molecular beam and proved planarity in both ground and lowest excited singlet states. The direction of the transition dipole moment of benzimidazole was determined by Schmitt et al.[7] from rotationally resolved electronic spectra of various isotopologues.

2. TECHNIQUES

2.1. Experimental Procedures. Benzimidazole (98%) was purchased from Aldrich and used without further purification. The experimental setup for the rotationally resolved laser induced fluorescence spectroscopy is described in detail elsewhere.[8] In brief, the laser system consists of a single frequency ring dye laser (Sirah Matisse DS) operated with Rhodamine 6G, pumped with 7 W of the 514 nm line of an Ar$^+$-ion laser (Coherent, Sabre 15 DBW). The dye laser output

Received: September 1, 2013
Revised: November 6, 2013
Published: November 6, 2013

was coupled into an external folded ring cavity (Spectra Physics Wavetrain) for second harmonic generation. The resulting output power was constant at about 20 mW during the experiment. The molecular beam was formed by coexpanding benzimidazole, heated to 190 °C, and 400 mbar of argon through a 200 μm nozzle into the vacuum chamber. The molecular beam machine consists of three differentially pumped vacuum chambers that are linearly connected by skimmers (1 mm and 3 mm, respectively) in order to reduce the Doppler width. The resulting resolution is 18 MHz (FWHM) in this setup. In the third chamber, 360 mm downstream of the nozzle, the molecular beam crosses the laser beam at a right angle. The imaging optics setup consists of a concave mirror (f = 25 mm) in a distance of 50 mm below the crossing of molecular beam and laser beam and two plano-convex lenses (f = 50 mm and f = 130 mm in distances of 50 mm and 70 mm, respectively, above the crossing) to focus the resulting fluorescence onto a photomultiplier tube (Thorn EMI 9863QB), which is mounted perpendicularly to the plane defined by the laser and molecular beam. The signal output was then discriminated and digitized by a photon counter and transmitted to a PC for data recording and processing. The relative frequency was determined with a quasi confocal Fabry–Perot interferometer. The absolute frequency was obtained by comparing the recorded spectrum to the tabulated lines in the iodine absorption spectrum.[9]

2.2. Computational Methods. *2.2.1. Quantum Chemical Calculations.* The anharmonic analysis of the vibrational spectrum allows for the determination of vibrational averaging effects on the rotational constants and inertial defects due to the individual vibrational motion.[10,11] Such an anharmonic analysis is implemented in the Gaussian program package.[13] The procedure for the calculation of cubic and of some of the quartic force constants utilizes numerical derivatives of the analytically determined Hessian with respect to the normal coordinates. We performed the analysis at the MP2 level with the 6-311G(d,p) basis set.

The vibrational/vibronic analyses of the hot band transitions have to rely on ground and excited state vibrational frequencies that have been obtained at the same level of theory. Assignment of excited state vibrations to the ground state vibrations has been made using the Duschinsky matrix:[12]

$$Q'' = SQ' + \vec{d} \tag{1}$$

where $\vec{d}$ is a displacement vector and S a rotation matrix, which rotates the coordinate system of one state into that of the other state. This matrix is called the Duschinsky matrix, which was obtained from the equilibrium geometries and Hessians using the approximate coupled cluster singles and doubles model (CC2), employing the resolution-of-the-identity approximation (RI).[14,15] Dunning's correlation correlation consistent polarized valence triple-ζ (cc-pVTZ) basis sets from the TURBOMOLE library[16−18] have been employed. The vibrational analysis for both states in order to obtain the respective Hessians was performed using numerical second derivatives with the NumForce script.[19]

2.2.2. Franck–Condon Analysis of Vibrationally Hot Electronic Spectra. We modified the existing program for Franck–Condon analysis of absorption and emission spectra[20] to cope with nonzero temperatures. The population of the ith ground state mode is given by the Boltzmann factor at the respective vibrational energy:

$$N_i = \frac{N g_i \, e^{-(h\nu_i/kT)}}{\sum_k g_k \, e^{-(h\nu_k/kT)}} \tag{2}$$

The sum over k in eq 2 runs over all ground state vibrations, their combinations, and their overtones. Radle and Beck gave an expression for the calculation of the Boltzmann factors in the case of harmonic vibrations:[21]

$$N_i = N g_i \, e^{-(h\nu_i/kT)} \prod_j (1 - e^{-(h\nu_j/kT)}) g_j \tag{3}$$

where the j products run over the $3N - 6$ normal modes. Using these populations, the absorption spectra of all ground state modes up to a maximum energy of 4000 cm^{-1} are calculated, keeping in mind the ν dependence of the intensities ($I \propto \nu^1$ for absorption and $I \propto \nu^3$ for emisson) in each of the spectra. A maximum vibrational quantum number for each mode of three, a maximum quantum number sum for all modes of four, and a maximum number of simultaneously excited modes of two was used in order to limit the amount of calculations. These numbers have been evaluated by gradually increasing them, until the changes in the spectra were much smaller than the experimental uncertanties. Finally, the spectra are weighted with the respective Boltzmann factor, summed up, and convoluted with a Gaussian line profile.

2.2.3. Fits of the Rovibronic Spectra Using Evolutionary Algorithms. The search algorithm employed for the fit of the rotationally resolved electronic spectra is an evolutionary strategy (ES) adapting normal mutations via a covariance matrix adaptation (CMA) mechanism. This (CMA-ES) algorithm was developed by Ostermeier and Hansen[22,23] and is designed especially for optimization on rugged search landscapes that are additionally complicated due to noise, local minima, and/or sharp bends. It belongs, like other search algorithms we also use, to the group of global optimizers that were inspired by natural evolution. For a detailed description of these evolutionary strategies, refer to refs 24 and 25. The cost (or fitness) function employed to judge the quality of the fit uses an inner product with special metric, as described in detail in ref 25

3. RESULTS

3.1. Results of the Quantum Chemical Calculations. *3.1.1. Results of the Anharmonic Second Order Møller–Plesset MP2 Calculations.* The vibrationally averaged rotational constants of benzimidazole have been calculated at the MP2/6-311G(d,p) level of theory, using the anharmonic option in the Gaussian program package. All rotational constants and harmonic and anharmonic wavenumbers are compiled in Table S1 of the Supporting Information. Benzimidazole, which has C_s symmetry, has a total of 39 vibrations, of which 12 are out-of-plane vibrations (Q_{39}–Q_{28}) and 27 are in-plane vibrations (Q_{27} – Q_1). Part of Table S1, Supporting Information, which contains the vibrational induced changes of the rotational constants, has been extracted and will be used in section 4.1 for the assignment of the vibrationally hot bands in the absorption spectrum of benzimidazole (Table 3). The anharmonic vibrational wavenumbers from this table are disregarded in the discussion, since most of them show completely unrealistic changes compared to the harmonic frequencies. The reason for this striking discrepancy for some modes is the deficiency of vibrational perturbation theory to handle vibrations, in which the harmonic term is not dominant. In the two-ring system

Table 1. CC2/cc-pVTZ Calculated and Experimental Wavenumbers of the 39 Normal Modes of the Ground and First Electronically Excited States of Benzimidazole along with the Respective Symmetry Labels and the Coefficients of the Duschinsky Matrix, Which Are Larger than 0.4

	S_0			S_1			
mode	sym	calcd	obsd[a]	sym	calcd	obsd[b]	Duschinsky
$Q_1(S_0)$	A′	3657		A′	3637		$Q_1(S_1) = -1.00Q_1(S_0)$
$Q_2(S_0)$	A′	3267		A′	3287		$Q_2(S_1) = -0.99Q_2(S_0)$
$Q_3(S_0)$	A′	3230		A′	3249		$Q_3(S_1) = -0.88Q_3(S_0)$
$Q_4(S_0)$	A′	3221		A′	3239		$Q_4(S_1) = -0.90Q_4(S_0)$
$Q_5(S_0)$	A′	3210		A′	3224		$Q_5(S_1) = -0.77Q_5(S_0)$
$Q_6(S_0)$	A′	3200		A′	3207		$Q_6(S_1) = -0.79Q_6(S_0)$
$Q_7(S_0)$	A′	1656	1631	A′	1589	1562	$Q_8(S_1) = -0.90Q_7(S_0)$
$Q_8(S_0)$	A′	1615	1612	A′	1515	1531	$Q_9(S_1) = -0.78Q_8(S_0)$
$Q_9(S_0)$	A′	1512		A′	1408	1420	$Q_{11}(S_1) = -0.55Q_9(S_0) + 0.53Q_{12}(S_0)$
$Q_{10}(S_0)$	A′	1500	1498	A′	1432	1437	$Q_{10}(S_1) = -0.60Q_{10}(S_0) - 0.70Q_9(S_0)$
$Q_{11}(S_0)$	A′	1481	1482	A′	1382	1381	$Q_{12}(S_1) = +0.70Q_{11}(S_0) - 0.56Q_{12}(S_0)$
$Q_{12}(S_0)$	A′	1449	1458	A′	1603	1611	$Q_7(S_1) = +0.45Q_{12}(S_0) + 0.55Q_{11}(S_0)$
$Q_{13}(S_0)$	A′	1391	1395	A′	1325	1321	$Q_{13}(S_1) = -0.80Q_{13}(S_0)$
$Q_{14}(S_0)$	A′	1323	1318	A′	1256	1257	$Q_{15}(S_1) = +0.80Q_{14}(S_0)$
$Q_{15}(S_0)$	A′	1290	1297	A′	1286	1291	$Q_{14}(S_1) = +0.89Q_{15}(S_0)$
$Q_{16}(S_0)$	A′	1269	1268	A′	1219	1221	$Q_{16}(S_1) = -0.91Q_{16}(S_0)$
$Q_{17}(S_0)$	A′	1195	1183	A′	1158		$Q_{17}(S_1) = -0.72Q_{17}(S_0) - 0.65Q_{18}(S_0)$
$Q_{18}(S_0)$	A′	1163	1154	A′	1140	1133	$Q_{18}(S_1) = +0.73Q_{18}(S_0) + 0.17Q_{20}(S_0)$
$Q_{19}(S_0)$	A′	1122	1115	A′	1054	1041	$Q_{19}(S_1) = +0.89Q_{19}(S_0)$
$Q_{20}(S_0)$	A′	1093	1079	A′	893		$Q_{21}(S_1) = -0.60Q_{20}(S_0) + 0.64Q_{21}(S_0)$
$Q_{21}(S_0)$	A′	1021	1021	A′	966	960	$Q_{20}(S_1) = -0.70Q_{21}(S_0) - 0.60Q_{20}(S_0)$
$Q_{22}(S_0)$	A′	928	939	A′	875	884	$Q_{22}(S_1) = -0.90Q_{22}(S_0)$
$Q_{23}(S_0)$	A′	881	869	A′	853	823	$Q_{23}(S_1) = +0.95Q_{23}(S_0)$
$Q_{24}(S_0)$	A′	780	776	A′	725	729	$Q_{24}(S_1) = +0.96Q_{24}(S_0)$
$Q_{25}(S_0)$	A′	617	620	A′	566	566	$Q_{25}(S_1) = +0.98Q_{25}(S_0)$
$Q_{26}(S_0)$	A′	542	543	A′	474	477	$Q_{26}(S_1) = -0.96Q_{26}(S_0)$
$Q_{27}(S_0)$	A′	407	414	A′	395	396	$Q_{27}(S_1) = -0.99Q_{27}(S_0)$
$Q_{28}(S_0)$	A″	953		A″	760	767	$Q_{28}(S_1) = -0.92Q_{28}(S_0)$
$Q_{29}(S_0)$	A″	925		A″	656		$Q_{30}(S_1) = -0.61Q_{29}(S_0) - 0.49Q_{30}(S_0)$
$Q_{30}(S_0)$	A″	855		A″	588		$Q_{32}(S_1) = +0.70Q_{30}(S_0) + 0.40Q_{34}(S_0)$
$Q_{31}(S_0)$	A″	847	852	A″	626		$Q_{31}(S_1) = +0.52Q_{31}(S_0) - 0.61Q_{33}(S_0)$
$Q_{32}(S_0)$	A″	767		A″	537	538	$Q_{33}(S_1) = -0.62Q_{32}(S_0) - 0.51Q_{34}(S_0)$
$Q_{33}(S_0)$	A″	750		A″	677	677	$Q_{29}(S_1) = -0.62Q_{33}(S_0) - 0.49Q_{29}(S_0)$
$Q_{34}(S_0)$	A″	648		A″	521		$Q_{34}(S_1) = -0.72Q_{34}(S_0) + 0.28Q_{33}(S_0)$
$Q_{35}(S_0)$	A″	582		A″	360	369	$Q_{36}(S_1) = -0.91Q_{35}(S_0)$
$Q_{36}(S_0)$	A″	458		A″	441		$Q_{35}(S_1) = -0.92Q_{36}(S_0)$
$Q_{37}(S_0)$	A″	431	433	A″	296	303	$Q_{37}(S_1) = -0.92Q_{37}(S_0)$
$Q_{38}(S_0)$	A″	255		A″	183	188	$Q_{38}(S_1) = -0.88Q_{38}(S_0)$
$Q_{39}(S_0)$	A″	229		A″	155	158	$Q_{39}(S_1) = -0.87Q_{39}(S_0)$

[a]From the DF spectra in ref 1. [b]From the LIF spectra in ref 1.

benzimidazole, several out-of-plane vibrations exhibit a double minimum potential, leading to completely unreliable vibrational frequencies after correction. Such a behavior of double minimum potentials in anharmonic corrections is known for large systems. For example, in the guanine-cytosine Watson–Crick pair, which is dominated by a Morse-like anharmonic potential along the hydrogen bond coordinate, anharmonic corrections have the right order of magnitude, while for the guanine-cytosine Hoogsteen base pair, a double minimum potential is found along the hydrogen bond, and anharmonic corrections are completely unreliable.[26] Nevertheless, the (small amplitude) distortion vectors describe the vibrational motion sufficiently exactly, in order to assess the vibrational contributions to the rotational constants.

3.1.2. Results of the Harmonic Second Order Coupled Cluster CC2 Calculations. The CC2/cc-pVTZ calculated vibrational wavenumbers in the electronic ground state S_0 and the first excited singlet state S_1 of benzimidazole are compiled in Table 1. They are compared to the laser induced fluorescence (LIF) and dispersed fluorescence (DF) data of Jalviste and Treshchalov.[1] For both states, a very close agreement between calculations and experiment has been found. For a planar molecule like benzimidazole, one would expect only in-plane motions to show up upon excitation from the vibrationless ground state. However, some very weak out-of-plane vibrations have been found in the spectra of Jalviste and Treshchalov,[1] which are unequivocally assigned on the basis of their wavenumbers. The excited state assignments to the mode numbers of the ground state have been made with the help of the Duschinsky matrix, which has been calculated from the respective Hessian of both electronic states. The largest elements of the Duschinsky are reproduced in Table 1 in

dx.doi.org/10.1021/jp408755q | J. Phys. Chem. A 2013, 117, 12812–12820

order to explain the motivation for the excited state assignments.

Figure 2 shows a simulation of the fluorescence emission spectrum of benzimidazole via the vibrationless origin 0,0 on

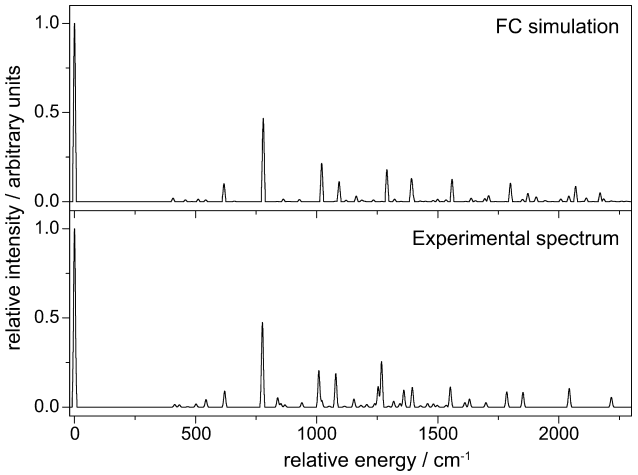

Figure 2. Comparison of the simulated Franck–Condon spectrum of fluorescence emission via the vibrationless origin 0,0 and the experimental DF spectrum of Jalviste and Treshchalov.[1]

the basis of the CC2/cc-pVTZ harmonic normal-mode analysis, using our program FCFit.[20]

The FC simulation is solely based on the CC2/cc-pVTZ calculated geometries and Hessians in both electronic states and contains no fitting parameters. The agreement between simulation and the experimental spectrum from Jalviste and Treshchalov[1] is reasonably good in this case. The experimental spectrum shown in Figure 2 has been reconstructed from the wavenumbers and intensities given in ref 1 using a bandwidth of 6 cm^{-1} for convolution of the stick spectrum with a Gaussian profile.

Although the intensities in fluorescence excitation spectra are much less reliable than in fluorescence emission due to saturation effects, changes in the excitation power, and interactions to other electronically excited states, we also tried to simulate the excitation spectrum. Several provisions have to be made. Since the absorption spectrum of benzimidazole shows signs of strong hot bands, changes had to be made to the FCFit program to include also transitions from excited vibrational levels in the electronic ground state. These changes to the program are described in section 2.2.2. It was not possible to simulate the intensities of all hot bands using a single temperature for the calculation of the occupation. The hot bands that emerge from the lowest vibrational level were simulated with a temperature of 100 K, while the highest one was reasonably well reproduced by a vibrational temperature of 400 K. In between the temperature was approximated assuming a linear relation between vibrational energy and temperature. This procedure is motivated by studies from Murakami et al. and Rademann et al.[27,28] Both groups observed an increase in the vibrational temperature with increasing vibrational energy. Murakami et al. attributed this effect to a decrease in the collision induced vibrational relaxation cross-section for vibrations high up in energy.[27]

Figure 3 shows the results of the simulation and the comparison to the experimental data from Jalviste and Treshchalov.[1] The wavenumbers of the transitions were

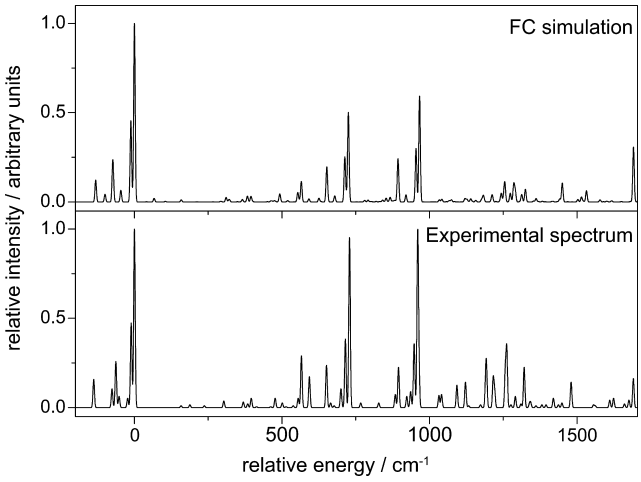

Figure 3. Comparison of the simulated Franck–Condon spectrum of fluorescence excitation and the experimental LIF spectrum of Jalviste and Treshchalov.[1]

obtained from Table 1 of ref 1. The respective intensities have been extracted from Figure 2 of the same publication. Regarding the fact that intensities in excitation spectra are much less reliable due to the effects mentioned before, the agreement between the experiment and the simulation is also reasonable.

3.2. High Resolution Spectra of Hot Bands of Benzimidazole. In total seven rotationally resolved electronic spectra of hot bands of benzimidazole were recorded and analyzed. They were fit using the CMA-ES algorithm (for a detailed description of the fit cf. section 2.2.3) with a rigid asymmetric rotor Hamiltonian and in-plane *ab*-selection rules including axis reorientation within the plane of symmetry. The band type of the rovibronic bands is given by the projection of the respective transition dipole moment (TDM) vector onto the principle axis system (PAS), which is described by the angle θ. In order to determine the absolute sign of θ for the investigated bands, we included axis reorientation into the analysis. The reorientation angle θ_T describes the rotation of the PAS in the ground state onto the PAS in the electronically excited state due to the altered equilibrium geometry. The effect of axis reorientation (in the literature also referred to as axis tilting or axis switching) upon change of the nuclear equilibrium configuration of the molecule is called the zero-order axis reorientation effect. It has consequences for the line strengths of the rotational transitions and has to be distinguished from the (higher order) vibrational contributions to the geometry changes, which are summarized in the Duschinsky effect. The axis switching matrix T is a pure rotation matrix, which transforms the matrix of direction cosines of a state A into that of a different state B: $\tilde{S}(\chi_A,\theta_A,\phi_A) = \tilde{T}\cdot\tilde{S}(\chi_B,\theta_B,\phi_B)$.[30] Comparison with the values from the literature yields a negative sign for both θ and θ_T for all bands. For a definition of the sign of θ and θ_T, refer to Figure 1.

The investigated hot bands consist of two groups of bands located (with respect to the electronic origin) at around −12 and −63 cm^{-1} (as of now named −12a, −12b, −63a, −63b, and −63c), and two single bands at −24 and −139 cm^{-1}. From the analysis of the rotational constants shown in Table 2, several facts become apparent. By comparison of the inertial parameters to the values determined for the electronic origin, published by Berden et al.[5] and Schmitt et al.,[7] we observe

dx.doi.org/10.1021/jp408755q | J. Phys. Chem. A 2013, 117, 12812–12820

Table 2. Experimentally Determined Molecular Parameters of the Investigated Hot Bands along with the Electronic Origin, Taken from ref 7[a]

	origin[7]	−12a	−12b	−24	−63a	−63b	−63c	−139
A'' (MHz)	3929.720(7)	3934.83(4)	3926.64(4)	3940.67(3)	3930.32(4)	3925.11(4)	3930.44(5)	3927.42(7)
B'' (MHz)	1679.259(3)	1679.39(2)	1678.17(2)	1679.86(1)	1680.94(1)	1681.97(1)	1678.92(2)	1678.19(3)
C'' (MHz)	1176.747(1)	1176.28(2)	1176.49(2)	1176.07(1)	1176.58(1)	1178.92(1)	1177.81(1)	1176.52(3)
ΔA (MHz)	−155.687(7)	−155.11(1)	−154.61(1)	−155.00(1)	−149.88(1)	−155.32(1)	−155.36(1)	−155.45(1)
ΔB (MHz)	−15.294(5)	−15.23(1)	−15.41(1)	−15.35(1)	−14.79(1)	−14.54(1)	−14.83(1)	−15.07(1)
ΔC (MHz)	−21.437(8)	−21.48(1)	−21.48(1)	−21.45(1)	−20.76(1)	−20.92(1)	−21.09(1)	−20.93(1)
A' (MHz)	3774.03(1)	3779.72(4)	3772.03(4)	3785.67(4)	3780.44(4)	3769.79(1)	3775.08(5)	3771.97(8)
B' (MHz)	1663.965(8)	1664.09(2)	1662.76(2)	1664.50(1)	1666.15(1)	1667.43(1)	1664.09(2)	1663.12(3)
C' (MHz)	1155.310(9)	1154.80(2)	1155.01(2)	1154.62(1)	1155.82(1)	1158.00(1)	1156.72(1)	1155.59(3)
I'' (amu Å^2)	−0.0866	+0.2738	−0.2880	+0.6268	0.2959	−0.5467	−0.5137	−0.2705
I' (amu Å^2)	−0.1889	+0.2233	−0.3679	+0.5833	0.2451	−0.7257	−0.6125	−0.5232
θ (deg)	−31.9(8)	−32.2(1)	−34.4(1)	−35.5(1)	−0.8(1)	−31.3(1)	−28.5(3)	−34.7(1)
θ_T (deg)	−0.72(1)	−0.52(1)	*b*	−0.72(1)[c]	−0.94(1)	*b*	*b*	−0.3(1)
τ (ns)	5.2(2)	7.1(1)	*b*	12.5(1)	5.2(1)	*b*	*b*	7.9(1)
ν (cm^{-1})	36021.38(1)	36009.43(1)	36009.19(1)	35997.28(1)	35958.20(1)	35958.10(1)	35957.00(1)	35882.44(1)
ν_{rel} (cm^{-1})		−11.95(2)	−12.12(2)	−24.10(2)	−63.18(2)	−63.28(2)	−64.38(2)	−138.94(2)

[a]The changes of the rotational constants are defined as $\Delta B_g = B_g' - B_g''$, with B_g as rotational constant with respect to the inertial axes $g = a,b,c$. ν_{rel} is the center frequency of the hot band relative to the undeuterated origin and τ is the excited state lifetime. [b]These values were set equal to the respective value of the first member of the group (12a and 63a). [c]This value was fixed to the value of the electronic origin.

Table 3. MP2/6-311 Calculated Vibrationally Averaged Rotational Constants for Several Benzimidazole Vibrations; in Parentheses, Their Changes Relative to the Zero-Point Averaged Rotational Constants at the r_0 Geometry Are Given

mode	$\tilde{\nu}$ (cm^{-1})	A″ (MHz)	B″ (MHz)	C″ (MHz)	ΔI (amu Å^2)
r_0		3875.6	1668.0	1166.4	−0.0866
Q_{21}	1025.8	3872.7 (−2.9)	1668.5 (+0.5)	1165.9 (−0.5)	+0.0748
Q_{22}	943.1	3874.8 (−0.8)	1668.3 (+0.3)	1166.0 (−0.4)	+0.0720
Q_{23}	890.9	3880.2 (+4.6)	1672.3 (+4.3)	1165.7 (−0.7)	+1.0897
Q_{28}	889.5	3871.2 (−4.4)	1662.9 (−5.1)	1166.4 (±0.0)	−0.6329
Q_{29}	872.2	3871.4 (−4.2)	1667.5 (−0.5)	1166.4 (±0.0)	−0.6295
Q_{30}	831.9	3870.3 (−5.3)	1667.9 (−0.1)	1166.5 (+0.1)	−0.3381
Q_{31}	806.6	3875.3 (−0.3)	1667.3 (−0.7)	1166.5 (+0.1)	−0.6302
Q_{24}	786.4	3874.5 (−1.1)	1667.3 (−0.7)	1165.6 (−0.8)	−0.6296
Q_{32}	725.3	3872.9 (−2.7)	1667.7 (−0.3)	1166.6 (+0.2)	−0.3239
Q_{33}	654.8	3874.9 (−0.7)	1667.4 (−0.6)	1166.6 (+0.2)	−0.3110
Q_{25}	623.7	3874.5 (−1.1)	1668.0 (±0.0)	1166.9 (+0.5)	−0.3272
Q_{34}	600.7	3873.5 (−2.1)	1667.6 (−0.4)	1166.8 (+0.4)	−0.3961
Q_{26}	547.7	3876.1 (+0.5)	1668.2 (+0.2)	1165.1 (−1.3)	+0.4324
Q_{35}	429.7	3872.8 (−2.8)	1667.7 (−0.3)	1166.7 (+0.3)	−0.3644
Q_{27}	410.3	3883.7 (+8.1)	1669.7 (+1.7)	1166.2 (−0.2)	+0.5506
Q_{36}	406.3	3874.2 (−1.4)	1666.8 (+0.8)	1167.0 (+0.6)	−0.5922
Q_{37}	374.8	3874.4 (−1.2)	1667.9 (−0.1)	1167.0 (+0.6)	−0.3855
Q_{38}	235.0	3875.0 (−0.6)	1667.1 (−0.9)	1167.2 (+0.8)	−0.5849
Q_{39}	210.9	3867.6 (−8.0)	1669.1 (+1.1)	1167.2 (+1.2)	−0.4712

Table 4. Difference between the Rotational Constants and Their Changes upon Electronic Excitation for the Vibrational Hot Bands; the Differences Are Defined As $X_{hotband} - X_{origin}$, $X = A, B, C$

	−12a	−12b	−24	−63a	−63b	−63c	−139
$\Delta A''$ (MHz)	+5.11	−3.08	+10.95	+0.60	−4.61	+0.72	−2.30
$\Delta B''$ (MHz)	+0.13	−1.09	+0.60	+1.68	+2.71	−0.34	−1.07
$\Delta C''$ (MHz)	−0.47	−0.26	−0.68	−0.17	+2.17	+1.06	−0.23
$\Delta\Delta A$ (MHz)	+0.58	+1.08	+0.69	+5.81	+0.37	+0.33	+0.24
$\Delta\Delta B$ (MHz)	−0.01	−0.12	−0.07	+0.50	+0.75	+0.46	+0.22
$\Delta\Delta C$ (MHz)	−0.04	−0.04	−0.01	+0.68	+0.52	+0.35	+0.51
$\Delta A'$ (MHz)	+5.69	−2.00	+11.64	+6.41	−4.24	+1.05	−2.06
$\Delta B'$ (MHz)	+0.12	−1.21	+0.53	+2.18	+3.46	+0.12	−0.85
$\Delta C'$ (MHz)	−0.51	−0.30	−0.69	+0.51	+2.69	+1.41	+0.28

dx.doi.org/10.1021/jp408755q | J. Phys. Chem. A 2013, 117, 12812−12820

slight deviations in the rotational constants of roughly between −5 and +10 MHz. These are too small to be caused by substitution as shown by Schmitt et al.[7] Furthermore, the size of the deviations is reproduced by the vibrational contributions to the rotational constants as shown in Table 3. Therefore, it seems safe to attribute all spectra observed to be hot bands of 1*H*2*H*-benzimidazole.

4. DISCUSSION

4.1. Assignment of the Hot Bands. The assignment of rotationally resolved electronic spectra of vibrational bands using anharmonic corrections to the inertial parameters was demonstrated by our group for 5-cyanoindole.[29] The general approach is as follows: first, the experimentally determined vibrational frequencies are compared to the results of harmonic calculations and a rough preselection of possible candidates is made. By this we are able to confine the number of normal modes, which have to be considered for a given vibrational band to those that are in a wavenumber interval of 30 cm^{-1} around the band of interest (in general between two or four). In the next step, the vibrational contributions to the rotational constants are taken into account and an assignment can be made.

In the present article, we investigate vibrationally hot bands of benzimidazole, which introduces significantly more complexity to the problem. As can be seen from a comparison of the calculated and measured vibrational contributions to the rotational constants in Tables 3 and 4, the deviations are too large to make an unequivocal assignment based only on them. They merely serve as guidance and have to be used in conjuncture with additional experimental evidence. Hence, we need to extract information from vibrationally resolved studies in the gas phase to constrain the number of vibrations to be considered. This, however, is the crucial point of the analysis: From the experiment, we have no information on the energetic positions of the respective vibrations in the ground and/or excited state. The only information we have is the shift relative to the electronic origin, which gives the difference in vibrational energy between the S_0 and S_1. However, a preselection can be made if we simulate the hot absorption spectra as described in the results section. On the basis of these results and the vibrational contributions in both electronic states, we can extract the information that will allow for an unequivocal analysis.

Vibrationally resolved spectra of benzimidazole in the S_1 state were presented by Jalviste and Treshchalov[1] and Jacoby et al.[2] By comparing the respective spectra of the two groups, we see a large number of vibrationally hot bands in the laser induced fluorescence spectrum of Jalviste and Treshchalov. According to the authors, hot bands were observed up to 729 cm^{-1} above the S_1 state, so we estimate 1000 cm^{-1} as an upper boundary for the vibrational energy in the ground state. Thereby, we can reduce the number of vibrations, which have to be considered from 39 to 19. In Table 3, all fundamental vibrations of benzimidazole within the first ∼1000 cm^{-1} are given along with the anharmonic contribution to the rotational constants and the inertial defect at the MP2/6-311G(d,p) level of theory; the complete list can be found in Table S1 of the Supporting Information. The normal modes are sorted according to their harmonic frequencies.

4.2. Assignment Based on the Vibrational Contributions to the Rotational Constants. In the following, we want to assign the hot bands using the information given by the vibrational contribution to the rotational constants. In Table 4 the vibrational contributions as extracted from the experimental spectra are given. $\Delta X''$ refers to the changes in the ground state, $\Delta X'$ to the changes in the electronically excited state, and $\Delta\Delta X$ to the changes induced by excitation ($\Delta X' - \Delta X'' = \Delta\Delta X$ for $X = A,B,C$). Before we turn to discuss the experimental findings, we should consider what we expect to find. First of all, transitions that start or end at a vibrationless level are not to be expected. This we can conclude as otherwise we would either not observe a hot band or would need vibrational bands below 140 cm^{-1} in the ground state, which are not present. For a diagonal transition, the same vibrational mode is excited in the electronic ground and in the excited state and the difference to the respective vibrationless state should be constant. Regarding Table 4, this means that $\Delta X''$ and $\Delta X'$ should be comparable, and the difference $\Delta\Delta X$ close to zero. The remaining difference would be a measure of how much the motion of the nuclei is influenced by the electronic excitation. Another possibility is that the vibrations in both states are not the same. In this case, we expect $\Delta\Delta X$ to deviate considerably from zero.

4.3. Vibronic Hot Bands around 0,0 −12 cm^{-1}. An energy level scheme, explaining the −12 and −24 cm^{-1} hot bands is shown in Figure 4. The vibrational frequencies in the figure are those from the CC2/cc-pVTZ calculations. The −12 cm^{-1} band systems is composed of two overlapping vibronic bands, whose center frequencies ν_0 are separated by 0.17 cm^{-1}. They will be discussed separately in the following. The spectrum and the best fit using the parameters given in Table 2 are shown in Figure 5.

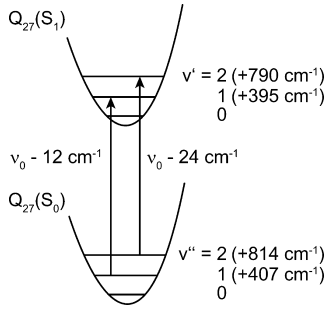

Figure 4. Energy level scheme for the hot vibrational bands at −12 (Q_{27}^1) and −24 cm^{-1} (Q_{27}^2). The vibrational frequencies shown in the graph are the CC2 calculated values from Table 1.

4.3.1. Band −12a. For the hot band −12a, an increase in the experimental *A* rotational constant of about 5 MHz is observed in both electronic states, while the vibrational contributions to *B* and *C* are small. Also because of the small changes of the vibrational contributions upon excitation ($\Delta\Delta X$ in Table 4), this band is very likely a diagonal transition. According to the calculated vibrationally averaged rotational constants shown in Table 3, the increase in *A* is mirrored best by Q_{27} calculated at 410 cm^{-1} in the S_0. This assignment is supported by the relative intensity in the vibrationally resolved spectrum, which is nearly 40% of that of the origin.[1] The Duschinsky matrix elements, given in Table 1 show that absorption from Q_{27} as ground state is dominated by the diagonal transition Q_{271}^1 (coefficient 0.99). The frequency in the S_1-state is shifted to lower wavenumbers from 407 to 395 cm^{-1} (frequencies from the CC2 calculations), corresponding to a shift of −12 cm^{-1}, which nicely reproduces the experimental finding.

dx.doi.org/10.1021/jp408755q | J. Phys. Chem. A 2013, 117, 12812−12820

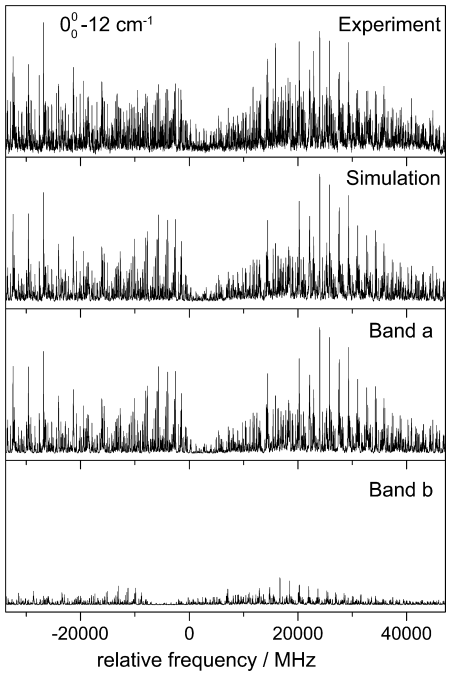

Figure 5. Rotationally resolved electronic spectra of the two vibronic bands centered around 0,0 −12 cm^{-1} along with the overall simulation using the best fit parameters from Table 2 and the simulations of the individual spectra.

4.3.2. Band −12b. Part of the intensity of the −12 transition is due to a second, overlapping band with an intensity of about 10% of the origin transition. The presence of a second weak band has first been detected from the autocorrelation of the experimental spectrum, in which a second peak at 5100 MHz appeared. Using the knowledge of the shift of the second band, we were able to fit also the second band using the evolutionary strategy. All $\Delta\Delta X$ are small, showing this band also to be a diagonal transition, with vibrational contributions of around ΔA = −3 MHz, ΔB = −1 MHz, and ΔC = 0 MHz. A possible assignment of this band is the diagonal transition Q_{36}^1. According to the CC2 calculated shift, this diagonal hot transition should appear at −16 cm^{-1}, unfortunately no experimental values for the fundamentals of this out-of-plane vibration are available for comparison. Also the vibrational contributions to the rotational constants and the negative inertial defect are in agreement with an out-of-plane vibration. Assignment to the diagonal Q_{35}^1 transition, which shows very similar vibrational contributions to the rotational constants, is excluded from comparison of experimental and calculated frequencies.

4.4. Vibronic Hot Band at 0,0 −24 cm^{-1}. Contrary to the band around −12 cm^{-1}, the band at −24 cm^{-1} consists only of a single vibronic band. The spectrum and the best fit using the parameters given in Table 2 are shown in the online Supporting Information. Changes of the rotational constants upon vibrational excitation of the band at 0,0 −24 cm^{-1} are approximately twice the ones observed for the band −12a, cf. Table 4. The same holds true for the inertial defect and the energetic shift. Hence, we assign this band to the diagonal transition Q_{27}^2 of the first overtone of Q_{27}.

4.5. Vibronic Hot Band System at 0,0 −63 cm^{-1}. The band system consists of three bands (−63a, −63b, and −63c), which are centered around 0,0 −63 cm^{-1}. As in the case of the bands around −12 cm^{-1}, we were guided first by an autocorrelation of the experimental spectrum in the determination of the number of vibronic bands contributing to this band system. Since the autocorrelation automatically yields the shift of the bands, the fit of the entire band system using the evolutionary approach, described in section 2.2.3, was straightforward. All three bands have very different vibrationally induced changes of the rotational constants, cf. Table 4. We discuss their assignments in full detail in the following sections. The spectrum is shown in Figure 6.

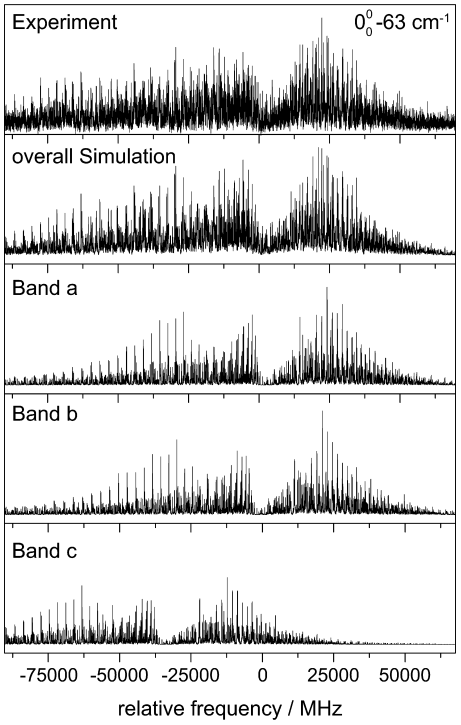

Figure 6. Rotationally resolved electronic spectra of the three vibronic bands centered around 0,0 −63 cm^{-1} along with the overall simulation using the best fit parameters from Table 2 and the simulations of the individual spectra.

4.5.1. Band −63a. The lowest energy band has a slightly positive inertial defect in both electronic states (+0.2959 (S_0) and +0.2451 (S_1)). A small positive inertial defect is regarded as evidence for the planarity of a molecule as stated by Oka.[31] Herschbach and Laurie divided the vibrational contributions to the inertial defect into in-plane and out-of-plane contributions. For the out-of-plane vibrations, a negative contribution to the inertial defect is found; for the in-plane vibrations, a positive one.[32] Thus, we expect the vibration to be in-plane both in the S_0 and the S_1 states. First, we note from the values given in Table 4 that the changes of the vibrational contributions due to electronic excitation ($\Delta\Delta X$) are much larger than for the bands at −12 and −24 cm^{-1}. We therefore conclude that the transition is nondiagonal and connects different modes in the hot ground and the excited states. The vibrationally induced changes of the rotational constants in the excited state are close to those calculated for mode Q_{27}. Hence, we propose a transition between combination bands to be responsible for the observed band: $Q_{27_1}^1 Q_{z_0}^1 Q_{x_1}^1 Q_{y_1}^1$. Because of symmetry reasons, either Q_x or Q_y necessarily have to be in-plane if Q_z is an out-of-plane vibration. The only in-plane vibration that can be sufficiently populated to account for such a strong hot band is Q_{26}. Plausible candidates are therefore combinations of Q_{26}

dx.doi.org/10.1021/jp408755q | J. Phys. Chem. A 2013, 117, 12812−12820

with a low frequency out-of-plane vibration: $Q_{270}^{1}Q_{z0}^{1}Q_{x1}^{0}Q_{261}^{0}$. Of all possible transitions, $Q_{270}^{1}Q_{340}^{1}Q_{371}^{0}Q_{261}^{0}$ has approximately the correct energy shift (-58 cm^{-1}).

4.5.2. Band −63b. The energetically following band shows a pronounced decrease in the A rotational constant for both the ground and the excited state and relatively large increases in B and C. As the differences of the rotational constants with respect to the origin are nearly the same for both electronic states (small values of $\Delta\Delta X$), we believe this band to be a diagonal transition. The large decrease in A is only mirrored by mode Q_{39}, computed to lie at 221 cm^{-1} (cf. Table 3). In a microwave study on benzimidazole, Velino et al. recorded two vibrationally induced satellites that were estimated to be located at 180 ± 30 and 210 ± 30 cm^{-1}.[3] The vibrational contribution to the rotational constants of the band at 180 ± 30 cm^{-1} are $\Delta A''$ = −8.71 MHz, $\Delta B''$ = +1.15 MHz, and $\Delta C''$ = +1.09 MHz. Comparison of these values to the entries in Table 3 shows a perfect agreement to mode Q_{39}. Therefore, we must have a combination band of the type $Q_{x1}^{1}Q_{391}^{1}$. The properties of Q_x are as follows: it should have a large increase in $\Delta A''$ and small increases in $\Delta B''$ and $\Delta C''$. The only band fitting to this pattern is Q_{27}. This is backed up by considerations of the intensity: The vibrational energy of the combination band $Q_{27}Q_{39}$ is 636 cm^{-1} (cf. the CC2 calculations in Table 1). According to Boltzmann for T = 460 K, the relative population of this combination is 14%, as observed in the spectrum. The CC2 calculated shift for this $Q_{271}^{1}Q_{391}^{1}$ transition is −80 cm^{-1}, the deviation from the observed −63 cm^{-1} can be attributed to anharmonic effects, which are not covered by the CC2 calculations.

4.5.3. Band −63c. The changes of the rotational constants for band −63c are not very pronounced for both electronic states. Given the small values of $\Delta\Delta X$, we again expect a diagonal transition. This would mean that we have a large number of possible modes: the in-plane mode Q_{25} and the out-of-plane modes Q_{33} and Q_{36}−Q_{38}. The inertial defects are of comparable size for the given candidates. Jalviste and Treshchalov presented the fluorescence emission spectrum of the band at 566 cm^{-1}, which shows a strong diagonal transition to 620 cm^{-1} in the ground state, showing this band to be due to Q_{25} excitation. According to the CC2 calculations shown in Table 1, the combination of Q_{25} and Q_{27} shows a shift upon excitation of exactly −63 cm^{-1}. We therefore assign the observed band −63c to the transition $Q_{251}^{1}Q_{271}^{1}$, although the excitation energy of this combination band is quite high and consequently should be less populated than found experimentally.

4.6. Vibronic Hot Band at 0,0 −138 cm^{-1}. The band at −138 cm^{-1}, shown in the Supporting Information, again seems to be a diagonal transition as can be seen from the small values of $\Delta\Delta X$. From its relative intensity (17%), we can deduce that it originates from a vibration not too high up in energy ($E_{vib} \approx$ 550 cm^{-1}). The changes in ΔB and ΔC are not very pronounced, but there is a noticeable decrease in ΔA. The most promising candidates are Q_{34} and Q_{35}. From the Duschinsky matrix, we see that for both vibrations there is a considerable decrease in the vibrational energy upon electronic excitation. This shift is −127 cm^{-1} (648−521 cm^{-1}) for Q_{34} and −222 cm^{-1} (360 −582 cm^{-1}) for Q_{35} (cf. the CC2 calculations in Table 1). So we rather believe that this band originates from Q_{34} as both the energies and that the vibrationally induced changes of the rotational constants fit and accordingly assign the band to Q_{341}^{1}.

5. CONCLUSIONS

A full assignment of the hot bands, observed in the excitation spectrum of benzimidazole was made on the basis of the vibrational averaging of the rotational constants combined with an analysis of the frequency shifts upon electronic excitation. The combination of anharmonic calculations at the MP2 level of theory for the electronic ground state, yielding vibrationally averaged rotational constants for all fundamental modes, combination bands, and overtones, with the analysis of the Duschinsky matrix, computed at the CC2 level of theory, leads to an unequivocal assignment of the hot bands. A Franck−Condon analysis of the fluorescence absorption and emission spectra further supports our assignments. The temperatures that had to be assumed in the simulation of the absorption spectrum were not uniform for all vibrations. Although the rotational temperatures in the molecular beam are nearly relaxed to the translational temperatures (<3 K), we found quite high temperatures for the vibrational degrees of freedom. The range of temperatures was 100 K for the lowest wavenumber vibrations and 400 K for the highest vibration considered in the simulation. Such a strong non-Boltzmann behavior of the cooling of vibrations in a molecular beam is not unusual and had been reported before, e.g., by Murakami et al.[27] and Rademann et al.[28]

■ ASSOCIATED CONTENT

Ⓢ Supporting Information

Complete list of harmonic and anharmonic frequencies and vibrationally averaged rotational constants from the MP2/6-311G(d,p) calculations as well as the rotationally resolved electronic spectra of the hot bands at 0,0 −24 cm^{-1}, and 0,0 −138 cm^{-1}. This material is available free of charge via the Internet at http://pubs.acs.org.

■ AUTHOR INFORMATION

Corresponding Author

*(M.S.) E-mail: mschmitt@uni-duesseldorf.de.

Present Address

†Quantum Nanophysics Group, Faculty of Physics, University of Vienna, Boltzmanngasse 5, 1190 Wien, Austria.

Notes

The authors declare no competing financial interest.

■ ACKNOWLEDGMENTS

We like to thank the Universitätsrechenzentrum Köln for the granted computing time on the HPC cluster Cheops. The financial support of the Deutsche Forschungsgemeinschaft (SCHM 1043/12) is gratefully acknowledged. We thank Christian Ratzer for experimental help in the early stage of the experiments.

■ REFERENCES

(1) Jalviste, E.; Treshchalov, A. Spectroscopy of Jet-Cooled Benzimidazole and Benzotriazole. *Chem. Phys.* **1993**, *172*, 325−338.

(2) Jacoby, C.; Roth, W.; Schmitt, M. A Comparison of Intermolecular Vibrations and Tautomerism in Benzimidazole, Benzotriazole and Their Binary Water Clusters. *Appl. Phys. B: Laser Opt.* **2000**, *71*, 643−649.

(3) Velino, B.; Trombetti, A.; Cané, E. Microwave Spectrum of Benzimidazole. *J. Mol. Spectrosc.* **1992**, *152*, 434−440.

(4) Cané, E.; Trombetti, A.; Velino, B.; Caminati, W. Assignment of the 278-nm Electronic Band System of Benzimidazole [1,3-

Benzodiazole] as $\pi^*-\pi$ by Rotational Band Contour Analysis. *J. Mol. Spectrosc.* **1991**, *150*, 222−228.
(5) Berden, G.; Meerts, W. L.; Jalviste, E. Rotationally Resolved Ultraviolet Spectroscopy of Indole, Indazole, and Benzimidazole: Inertial Axis Reorientation in the $S_1(^1L_b)S_0$ Transitions. *J. Chem. Phys.* **1995**, *103*, 9596−9606.
(6) Duschinsky, F. On the Interpretation of Electronic Spectra of Polyatomic Molecules. *Acta Physicochim. URSS* **1937**, *7*, 551−577.
(7) Schmitt, M.; Krügler, D.; Böhm, M.; Ratzer, C.; Bednarska, V.; Kalkman, I.; Meerts, W. L. A Genetic Algorithm Based Determination of the Ground and Excited (^1L_b) State Structure and the Orientation of the Transition Dipole Moment of Benzimidazole. *Phys. Chem. Chem. Phys.* **2006**, *8*, 228−235.
(8) Schmitt, M.; Küpper, J.; Spangenberg, D.; Westphal, A. Determination of the Structures and Barriers to Hindered Internal Rotation of the Phenol-Methanol Cluster in the S_0 and S_1 States. *Chem. Phys.* **2000**, *254*, 349−361.
(9) Gerstenkorn, S.; Luc, P. *Atlas du spectre d'absorption de la molécule d'iode 14800--20000 cm^{-1}*; CNRS: Paris, 1986.
(10) Barone, V. Anharmonic Vibrational Properties by a Fully Automated Second-Order Perturbative Approach. *J. Chem. Phys.* **2005**, *122*, 014108.
(11) The inertial defect measures the planarity of a molecule and is defined as $\Delta I = I_c - I_a - I_b$. For planar molecules, it is zero; for nonplanar molecules, it becomes negative.
(12) The normal coordinates Q′ of the excited state and Q″ of the ground state are related by the linear orthogonal transformation given by Duschinsky.[6]
(13) Frisch, M. J.; Trucks, G. W.; Schlegel, H. B.; Scuseria, G. E.; Robb, M. A.; Cheeseman, J. R.; Montgomery, J. A., Jr.; Vreven, T.; Kudin, K. N.; Burant, J. C.; et al. *Gaussian 03*, revision a.1; Gaussian, Inc.: Pittsburgh, PA, 2003.
(14) Ahlrichs, R.; Bär, M.; Häser, M.; Horn, H.; Kölmel, C. Electronic Structure Calculations on Workstation Computers: The Program System Turbomole. *Chem. Phys. Lett.* **1989**, *162*, 165−169.
(15) Dunning, T. H., Jr. Gaussian Basis Sets for Use in Correlated Molecular Calculations. I. The Atoms Boron Through Neon and Hydrogen. *J. Chem. Phys.* **1989**, *90*, 1007−1023.
(16) Hättig, C.; Weigend, F. CC2 Excitation Energy Calculatons on Large Molecules Using the Resolution of the Identity Approximation. *J. Chem. Phys.* **2000**, *113*, 5154−5161.
(17) Hättig, C.; Köhn, A. Transition Moments and Excited-State First-Order Properties in the Coupled Cluster Model CC2 Using the Resolution-of-the-Identity Approximation. *J. Chem. Phys.* **2002**, *117*, 6939−6951.
(18) Hättig, C. Geometry Optimizations with the Coupled-Cluster Model CC2 Using the Resolution-of-the-Identity Approximation. *J. Chem. Phys.* **2002**, *118*, 7751−7761.
(19) *TURBOMOLE V6.3*, 2012. http://www.turbomole.com.
(20) Böhm, M.; Tatchen, J.; Krügler, D.; Kleinermanns, K.; Nix, M. G. D.; LeGreve, T. A.; Zwier, T. S.; Schmitt, M. High-Resolution and Dispersed Fluorescence Examination of Vibronic Bands of Tryptamine: Spectroscopic Signatures for L_a/L_b Mixing near a Conical Intersection. *J. Phys. Chem. A* **2009**, *113*, 2456−2466.
(21) Radle, W. F.; Beck, C. A. An Experimental Study of the Near Ultraviolet Absorption Spectrum of Benzene. *J. Chem. Phys.* **1940**, *8*, 507−513.
(22) Ostermeier, A.; Gawelczyk, A.; Hansen, N. Step-Size Adaptation Based on Non-Local Use of Selection Information. In *Lecture Notes in Computer Science: Parallel Problem Solving from Nature (PPSN III)*; Springer: New York, 1994; pp 189−198.
(23) Hansen, N.; Ostermeier, A. Completely Derandomized Self-Adaptation in Evolution Strategies. *Evol. Comput.* **2001**, *9* (2), 159−195.
(24) Brand, C.; Oeltermann, O.; Pratt, D. W.; Weinkauf, R.; Meerts, W. L.; van der Zande, W.; Kleinermanns, K.; Schmitt, M. Rotationally Resolved Electronic Spectroscopy of 5-Methoxyindole. *J. Chem. Phys.* **2010**, *133*, 024303−1−024303−11.
(25) Meerts, W. L.; Schmitt, M. Application of Genetic Algorithms in Automated Assignments of High-Resolution Spectra. *Int. Rev. Phys. Chem.* **2006**, *25*, 353−406.
(26) Bende, A.; Bogdan, D.; Muntean, C. M.; Morari, C. Localization and Anharmonicity of the Vibrational Modes for GC Watson−Crick and Hoogsteen Base Pairs. *J. Mol. Model.* **2011**, *17*, 3265−3274.
(27) Murakami, J.; Kaya, K.; Ito, M. Multiphoton Ionization Spectra of Benzene, Fluorobenzene, and Chlorobenzene Resonant with S_0-S_1 Transitions by Use of Nozzle Beam Method. *J. Chem. Phys.* **1980**, *72*, 3263−3270.
(28) Rademann, K.; Brutschy, B.; Baumgärtel, H. Electronic Spectroscopy of Fluorobenzene van der Waals Molecules by Resonant Two-Photon Ionization. *Chem. Phys.* **1983**, *80*, 129−145.
(29) Brand, C.; Happe, B.; Oeltermann, O.; Wilke, M.; Schmitt, M. High Resolution Spectroscopy of Several Rovibronically Excited Bands of 5-Cyanoindole: The Effect of Vibrational Averaging. *J. Mol. Struct.* **2012**, *1044*, 21−25.
(30) Hougen, J. T.; Watson, J. K. G. Anomalous Rotational Line Intensities in Electronic Transitions of Polyatomic Molecules: Axis-Switching. *Can. J. Phys.* **1965**, *43*, 298−320.
(31) Oka, T. On Negative Inertial Defect. *J. Mol. Struct.* **1995**, *352/353*, 225−233.
(32) Herschbach, D. R.; Laurie, V. W. Influence of Vibrations on Molecular Structure Determinations. III. Inertial Defects. *J. Chem. Phys.* **1964**, *40*, 3142−3153.